



P84/ZIF-8 mixed matrix membranes for pervaporation dehydration of isopropanol

Sina Fazlifard^a, Nima Allahgholi^a, Toraj Mohammadi^{a,*}, Omid Bakhtiari^b

^aResearch and Technology Center for Membrane Processes, Iran University of Science & Technology (IUST), Narmak, Tehran, Iran, Tel./Fax: +98 21 77240051; emails: torajmohammadi@iust.ac.ir (T. Mohammadi), sina_fazli@chemeng.iust.ac.ir (S. Fazlifard), nimanima67@yahoo.com (N. Allahgholi)

^bDepartment of Chemical Engineering, Razi University, Kermanshah, Iran, email: omidbakhtiari@iust.ac.ir

Received 17 November 2015; Accepted 14 May 2017

ABSTRACT

In this study, zeolitic imidazolate framework-8 (ZIF-8) nanoparticles were successfully synthesized and embedded into P84 polymeric matrix to prepare P84/ZIF-8 mixed matrix membranes (MMMs) to investigate the effect of ZIF-8 addition as a new filler on dehydration performance of the P84 polymeric membrane. MMMs were evaluated using pervaporation (PV) dehydration of isopropanol (IPA). Synthesized ZIF-8 nanoparticles and MMMs were characterized by X-ray diffraction, scanning electron microscopy, Fourier transform infrared spectroscopy and swelling study. PV performance of the prepared MMMs with various ZIF-8 loadings such as 2.5, 5, 7.5 and 10 wt%, for IPA dehydration was investigated at 25°C. The results showed that for the ZIF-8/P84 MMMs at the optimum loading (5 wt%), the total flux increases 11% without any reduction in separation factor. The present work demonstrates good PV performance of the ZIF-8 incorporated MMMs for dehydration of IPA.

Keywords: Mixed matrix membrane; Nanostructured metal–organic framework; Pervaporation; P84; ZIF-8

1. Introduction

Separation of aqueous/organic mixtures is an important process in many industries [1]. Alcohol/water mixtures are widely used as cleansing agent in different industrial fields. The waste alcohol has to be recycled and recovered because of environmental economical point of view [2]. Distillation, absorption and adsorption are used to separate alcohol from alcohol/water mixtures, but all of these processes consume huge amount of energy [3].

In last decades, new various separation techniques have been studied. Hierarchical composite adsorbents, nanostructured photocatalysts, capacitive deionization and membrane separation are new methods investigated for water purification in recent years [4–8]. Using membrane processes for separation of alcohol from water is a common way due to their benefits such as saving energy, low costs and scaling up

easily. Pervaporation (PV) is one of the membrane processes that have achieved popularity as an effective process for close-boiling and azeotropic mixtures separation. It is new technology with good performance and selectivity. Hence, PV is a reliable process to separate alcohol from aqueous mixtures [2,3,9–12].

In the past years, lots of activities have been performed to make high performance PV membranes for alcohols separation. A good PV membrane should have high stability, permeability and selectivity. Inorganic membranes have good stability and performance, but their applications are restricted because of their costs and frangibility. On the other hand, polymeric membranes have limited performance because of their trade-off between selectivity and permeability [13–16].

Recently, various nanofillers such as different types of graphene, SiO₂ and carbon nanotubes have been used to improve properties of various polymers through different strategies [17–22]. Different polymeric membranes have been rectified with inorganic fillers such as carbon molecular

* Corresponding author.

sieves, zeolites and carbon nanotubes to provide characteristics of both organic and inorganic membranes [23–28]. Mixed matrix membranes (MMMs) are homogenous combinations of filler particles in polymeric matrixes [29]. Researchers have recently produced new type of fillers called metal organic frameworks (MOFs). MOFs are nanostructured materials with higher porosity than their inorganic counterparts and zeolites [26]. Many researchers have been performed for making new MMMs using MOFs for PV. Amirilargani and Sadatnia [30] incorporated zeolitic imidazolate framework-8 (ZIF-8) into polyvinylalcohol for PV dehydration of IPA. They showed that total flux increases, while separation factor decreases by adding ZIF-8. Hua et al. [3] used ZIF-90/P84 MMMs for dehydration of IPA. They reported that water flux and water selectivity enhances with increasing ZIF-8 content in mixed MMMs. Polybenzimidazol (PBI)/ZIF-8 as another MMM was used for PV dehydration of alcohols by Shi et al. [31], they presented enhanced in permeability without significant reduction in selectivity. MOF HKUST-1 was also incorporated into polyimide for PV. It showed increasing flux and decreasing selectivity with filler loading [32]. ZIF-71/PEBA MMMs were used for recovery of biobutanol [33]. Kang et al. [34] synthesized ZIF-7/chitosan MMMs for separation of water/alcohol mixtures. They indicated that separation factor and flux of MMMs exceed upper limit of chitosan-based membranes reported previously.

ZIF-8 is a member of MOFs family with a small pore size of 3.4 Å and cavity size of 11.6 Å. ZIF-8 is an attractive MOF because of its similarity to zeolites such as porosity, uniform pore size, and superior thermal and chemical stability [30]. ZIF-8 has the right pore size for dehydration of alcohols like IPA. The pore size of the ZIF-8 is larger than water kinetic diameter (2.65 Å) and smaller than kinetic diameter of IPA (4.5 Å), this feature can be used for enhancing dehydration performance of MMMs [3]. Fig. 1(a) shows ZIF-8 structure. Hydrogen atoms are shown by red, blue and green balls and zinc metal tetrahedral coordination is figured by green pyramids. ZIF-8 has an Sodalite (SOD) topology. Fig. 1(b) shows SOD topology for ZIF-8 [35].

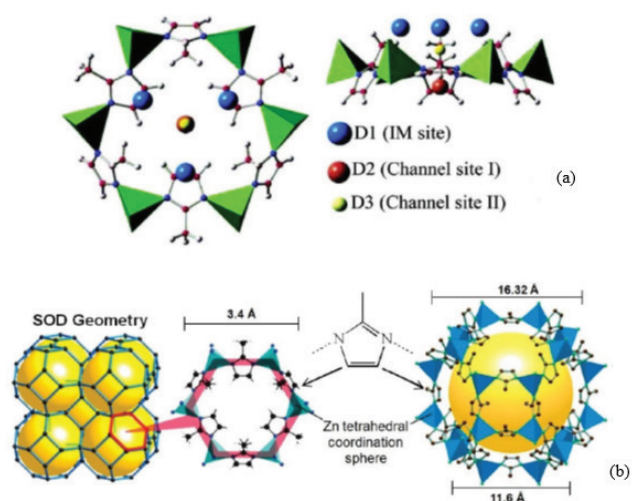


Fig. 1. ZIF-8 structure (a) schematic structure of ZIF-8 (b) SOD topology of ZIF-8 [35].

Polyimides have shown good film-forming property and notable separation performance in PV dehydration process (14). Polyimides have become as capable materials for PV membranes because of their superior thermal and chemical resistance, high mechanical strength, easy syntheses, processing and modifications [12]. To our knowledge, incorporation of ZIF-8 nanoparticles in P84 matrix for PV process has not been reported yet. The main aim of this research was to investigate the effect of ZIF-8 addition as new filler to P84 MMMs on their dehydration performance. P84 structure of the repeating unit is presented in Fig. 2 [3].

As a result, ZIF-8 was first synthesized and characterized. Afterward the synthesized ZIF-8 nanoparticles were incorporated into P84 matrix. The prepared MMMs were also characterized and evaluated in IPA dehydration.

2. Experimental setup

2.1. Materials

The P84 polymer powder was purchased from HP Polymer GmbH, Austria. Zinc nitrate hexahydrate ($Zn(NO_3)_2 \cdot 6H_2O$; 98%) was purchased from Riedel-de Haën (Germany). 2-Methylimidazole (Hmim; 99%) and 1-methyl-2-pyrrolidone (NMP; 99.5%) were purchased from Merck (Germany). All of the materials were used without further purification.

2.2. Synthesis of ZIF-8 nanoparticles

ZIF-8 nanoparticles were synthesized based on the method reported in literature [36]. For synthesizing of ZIF-8, $Zn(NO_3)_2 \cdot 6H_2O$, Hmim and methanol were employed in a molar ratio of approximately 1:8:700. First, a solution of 5.92 g of Hmim in 126 mL of methanol and another solution of 2.71 g of $Zn(NO_3)_2 \cdot 6H_2O$ in 126 mL of methanol were prepared and mixed at room temperature. The resultant solutions were then mixed for 1 h. The nanoparticles were collected via centrifugation and washing with methanol twice and with chloroform once. ZIF-8 nanoparticles were dried under vacuum at 120°C for 24 h [37,38] and stored dry for further analysis. Yield of the ZIF-8 synthesis was 70% based on zinc.

2.3. Membrane preparation

The polymers and the filler (with their wt% according to Table 1) were activated at 120°C under vacuum overnight to remove any adsorbed adsorbents like water and/or volatile organic compounds. Afterward ZIF-8 nanoparticles were dispersed in NMP. Then, 10% of desired amount of the polymer was added to the ZIF-8/NMP suspension and stirred overnight to make good adhesion between the filler particles and the polymer. After that, the remaining polymer was dissolved

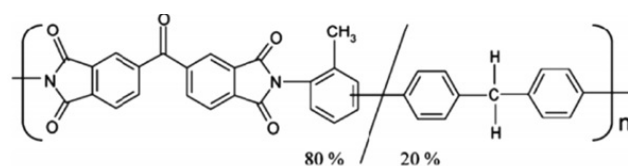


Fig. 2. P84 structure of the repeating unit [3].

in the previously prepared solution and stirred for 24 h. The solution was finally degassed under vacuum (−0.04 MPa, 120°C) for 4 h. It must be mentioned that due to low vapor pressure of NMP within degassing the solvent vaporization was negligible.

Certain volumes of the solution were selected in such manner that after solvent evaporation, thin films of 40–60 μm (Mitutoyo digital micrometer, 1 μm accuracy) were formed on the glass mold. After peeling of the nascent membranes, they were placed between the two stainless steel meshes in an oven to be treated. The membranes were hold at about 180°C for 12 h to remove the residual solvent. The ZIF-8 loading in the membranes was calculated using the following equation:

$$\text{Particles loading wt.\%} = \frac{\text{particles weight}}{\text{particles weight} + \text{polymer weight}} \times 100 \quad (1)$$

2.4. Characterization

2.4.1. X-ray diffraction (XRD)

The crystallographic structure of the ZIF-8 nanoparticles was studied by using a SIE-MENS, D5000 (Germany). The X-rays of 1.54 Å wavelengths were generated by a Cu Kα radiation source. The angle of diffraction (2θ) was varied from 5° to 40°. The crystallite size was calculated by the Scherrer method [39] using Eq. (2):

$$d = \frac{K\lambda}{B_{1/2} \cos(\theta_b)} \quad (2)$$

where d is the crystal size, θ_b is the Bragg angle, λ is the wavelength of the X-ray ($\lambda = 1.54 \text{ \AA}$), $B_{1/2}$ is the full width of the peak at half intensity and K is the unit cell geometry dependent constant chosen as 0.9.

2.4.2. Fourier transform infrared spectroscope (FTIR)

FTIR spectroscope pattern of the synthesized ZIF-8 nanoparticles and membranes were recorded using a PerkinElmer Spectrum between 700 and 3,700 cm^{-1} .

2.4.3. Scanning electron microscope (SEM) and energy dispersive spectrometry

Morphology of the prepared ZIF-8 nanoparticles and membranes was analyzed using a VEGA III TESCAN SEM. Elemental mapping was taken using an energy dispersive X-ray (EDX). The membrane samples were prepared by fracturing in liquid nitrogen.

Table 1
Wt% of materials used for membrane preparation

| Material | Wt% |
|----------|----------------------------------|
| NMP | 90 |
| P84 | 10 |
| ZIF-8 | 2.5, 5, 7.5, 10 (of the polymer) |

2.4.4. Swelling study

The membranes were dried completely at 60°C for 12 h and weighed by a digital microbalance (Sartorius AG, Germany) sensitive to ±0.1 mg. Then, these membranes were immersed in 15 wt% water containing feed mixtures in a sealed vessel at 25°C for 48 h. The swollen membranes were weighed immediately after blotted with filter papers. The percentage degree of swelling (DS) of the membranes was calculated using the following equation:

$$\text{Degree of swelling (DS\%)} = \left(\frac{W_s - W_d}{W_d} \right) \times 100 \quad (3)$$

where W_s and W_d are mass of the swollen and dried membranes, respectively.

2.5. Pervaporation experiments

The experiments were performed at 25°C using a PV setup as shown in Fig. 3. Feed mixtures of IPA–water were prepared and hold in a feed tank with net capacity of 500 cm^3 . Net provided membrane area in contact with the feed was 21 cm^2 . The membrane permeation side was evacuated using a vacuum pump (Vactorr, 25, USA). The system was stabilized for 4 h before the sample collection. A cold trap immersed in liquid nitrogen was employed to trap the permeated vapor via freezing. Water concentration of the feed and the permeate were measured via an Abbe Refractometer. Concentration was calculated by comparing the recorded refractive index values with a calibration curve. The membranes permeation properties were characterized using total flux (J), separation factor (α) and pervaporation separation index (PSI) by the following equations, respectively:

$$J = \frac{m}{A \times t} \quad (4)$$

$$\alpha = \frac{y/(1-y)}{x/(1-x)} \quad (5)$$

$$\text{PSI} = J(\alpha - 1) \quad (6)$$

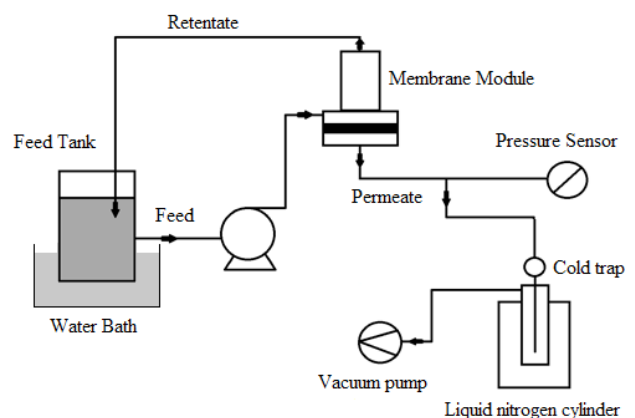


Fig. 3. Schematic diagram of the setup used for PV experiments.

where m is the mass of permeate (g), A is the effective membrane surface area (m^2) and t is the permeation time (h). x and y are water weight fractions in feed and permeate, respectively.

3. Results and discussion

3.1. ZIF-8 nanoparticles characterization

3.1.1. XRD

The synthesized ZIF-8 nanoparticles were characterized by XRD and Fig. 4 shows the XRD pattern. All main peaks at 2θ of 7.3° , 10.5° , 12.7° , 16.4° and 18.1° from the XRD pattern match well with the published XRD pattern of the ZIF-8 sample in literature [40]. This confirms that the prepared nanoparticles are certainly ZIF-8. The crystallite size was calculated by the Scherrer method is 24.6 nm.

3.1.2. FTIR

The synthesized ZIF-8 nanoparticles were characterized by FTIR and Fig. 5 shows the FTIR spectrum. FTIR spectrum of ZIF-8 sample in literature [40] is similar to the spectrum of the synthesized nanoparticles confirming that the prepared nanoparticles are certainly ZIF-8.

3.1.3. SEM

SEM image of the synthesized ZIF-8 nanoparticles is shown in Fig. 6. As observed, the crystals do not display a distinct morphology and the majority of ZIF-8 nanoparticles have diameters smaller than 60 nm.

3.2. MMMs characterization

3.2.1. XRD

The fabricated MMMs were characterized by XRD and Fig. 7 presents the XRD pattern of MMMs. XRD patterns

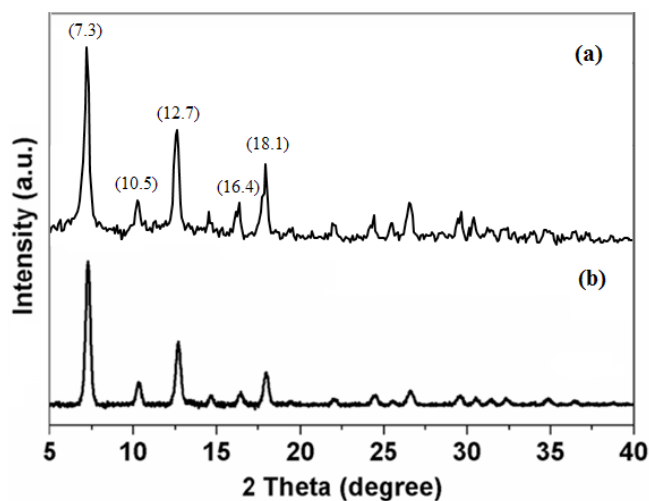


Fig. 4. XRD pattern of (a) the synthesized ZIF-8 nanoparticles and (b) reported in literature.

show sharp peaks of ZIF-8 confirming that ZIF-8 nanoparticles are properly mixed with the polymer.

3.2.2. FTIR

Fig. 8 shows FTIR spectrum of the neat polymer, ZIF-8 and fabricated MMMs. Two peaks at $2,923$ and $2,854$ cm^{-1} were due to symmetric and asymmetric stretching vibration

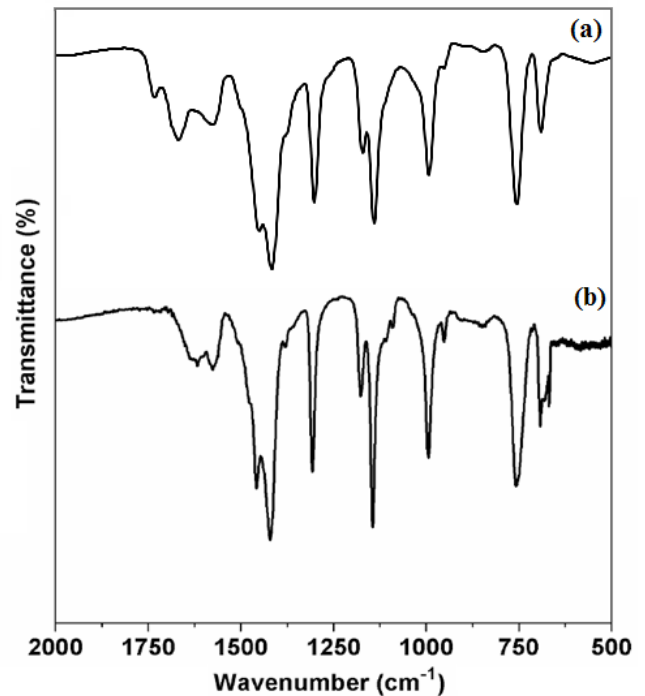


Fig. 5. FTIR spectrum of (a) the synthesized ZIF-8 nanoparticles and (b) reported in literature.

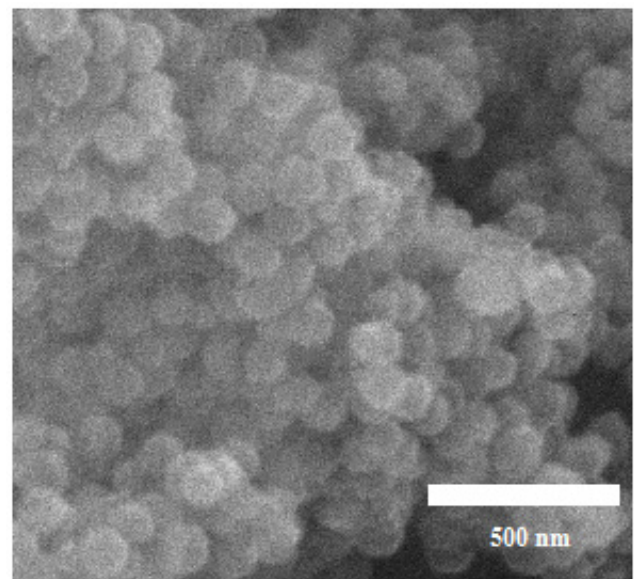


Fig. 6. SEM image of the synthesized ZIF-8 nanoparticles.

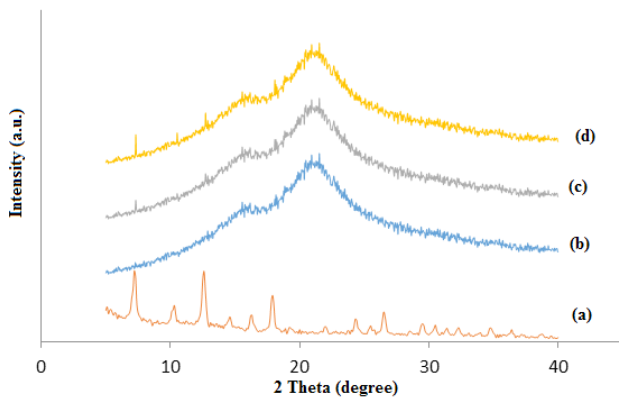


Fig. 7. XRD pattern of (a) ZIF-8 nanoparticles, prepared P84/ZIF-8, (b) neat P84, (c) 2.5 wt% and (d) 7.5 wt%.

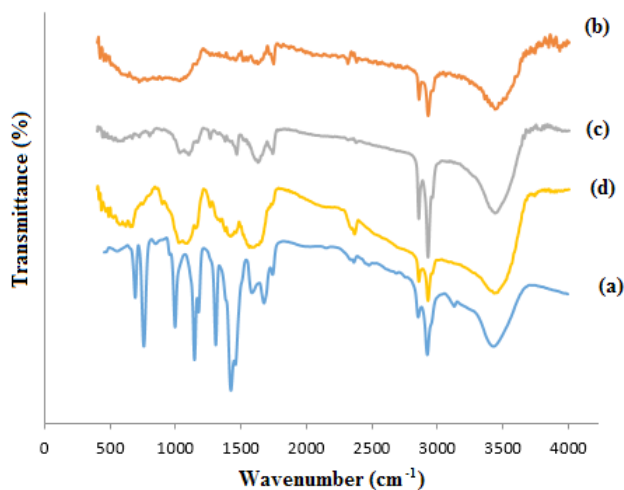


Fig. 8. FTIR spectrum of (a) ZIF-8 nanoparticles, prepared P84/ZIF-8, (b) neat P84, (c) 2.5 wt% and (d) 7.5 wt%.

of CH₂ groups. Characteristic peak at 1,737 cm⁻¹ is because of imide functional group. The existence of imide was confirmed by the peak at 721 cm⁻¹. At 1,078 cm⁻¹ a peak was due to benzene rings for the neat P84 membrane [41]. The peaks at 1,140 and 757 cm⁻¹ for ZIF-8 nanoparticles were due to the C–N and C–H bond, respectively.

3.2.3. SEM

Cross-sectional SEM images of the prepared P84/ZIF-8MMMs are presented in Fig. 9. The images show a homogeneous dispersion of the ZIF-8 nanoparticles in the polymer matrix and good adhesion between the two phases. No obvious particles agglomeration and voids formation are observed for most filler loadings and only when the ZIF-8 loading increases to 10 wt% some minor agglomeration of the ZIF-8 nanoparticles can be detected as shown in Fig. 8(e).

In Fig. 10, dispersion of ZIF-8 nanoparticles was investigated by mapping Zn element with using of EDX since zinc element exists only in ZIF-8 structure. Homogeneous scattering of Zn element confirms uniform dispersion of ZIF-8

in the P84 matrix at low loading but with increasing ZIF-8 loading, these particles become close together resulting in less homogeneity.

3.2.4. Swelling

In PV, membrane swelling has significant effect on diffusion of feed molecules permeating through the membrane. The DS depends on feed and membrane properties, such as chemical compositions of feed and membrane, physicochemical properties and microstructure of the membrane. The percentage DS of the prepared MMMs in the IPA/water (85/15 by weight) solution is illustrated in Fig. 11. As shown, the neat P84 membrane shows lower DS compared with the MMMs prepared with different loadings of the ZIF-8 nanoparticles. Addition of the ZIF-8 nanoparticles into the P84 matrix may have two effects on DS. Addition of ZIF-8 may increase the membrane free volume via interrupting the molecular organization of the polymer chains [30]. On the other hand, addition of ZIF-8 with hydrophobic nature into the hydrophilic P84 matrix results in reduction of DS [30]. However, DS of the MMMs increases by increasing the ZIF-8 loading. Aggregation of the ZIF-8 nanoparticles increases the free volume of MMMs via reduction of the membrane compactness and as a result feed molecules can pass through the membrane more easily.

3.3. PV performance

3.3.1. Effect of ZIF-8 loading on PV performance of MMMs

Fig. 12 shows the effect of ZIF-8 loading on PV performance of the prepared MMMs for dehydration of 85 wt% IPA aqueous solution at 25°C. As observed, total flux significantly increases with increasing the ZIF-8 loading in the MMMs. At the same time, separation factor is constant for the MMMs with the ZIF-8 loadings <5 wt%, but with increasing the ZIF-8 loading >5 wt%, separation factor decreases. Increasing total flux by increasing the ZIF-8 loading can primarily be the result of interfacial voids between the ZIF-8 nanoparticles and the P84 polymer matrix. Also, sorption of IPA molecules increases by increasing the ZIF-8 loading in the MMMs because of its super hydrophobicity, and this leads to the higher IPA permeation flux. Increasing the ZIF-8 content to the higher loadings significantly increases permeation flux, while decreases separation factor dramatically. This can be due to the interfacial voids and the ZIF-8 nanoparticles agglomeration [30,31]. Also, as shown in the SEM images, the ZIF-8 nanoparticles are agglomerated at the higher ZIF-8 loadings. Agglomeration of the ZIF-8 nanoparticles increases the polymer free volume and thus the feed molecules can permeate through the membrane more easily. As a measure of membrane separation performance, PSI was also calculated for the prepared MMMs as presented in Fig. 13. As shown, PSI values enhance with increasing the ZIF-8 loading up to 5 wt% and then reduce dramatically by increasing to 10 wt%. This reduction can be the result of the significantly reduced separation factor due to the agglomeration. As shown, the membrane with 5 wt% ZIF-8 loading has the highest PSI value compared with the other membranes and exhibits the best performance for PV dehydration of IPA.

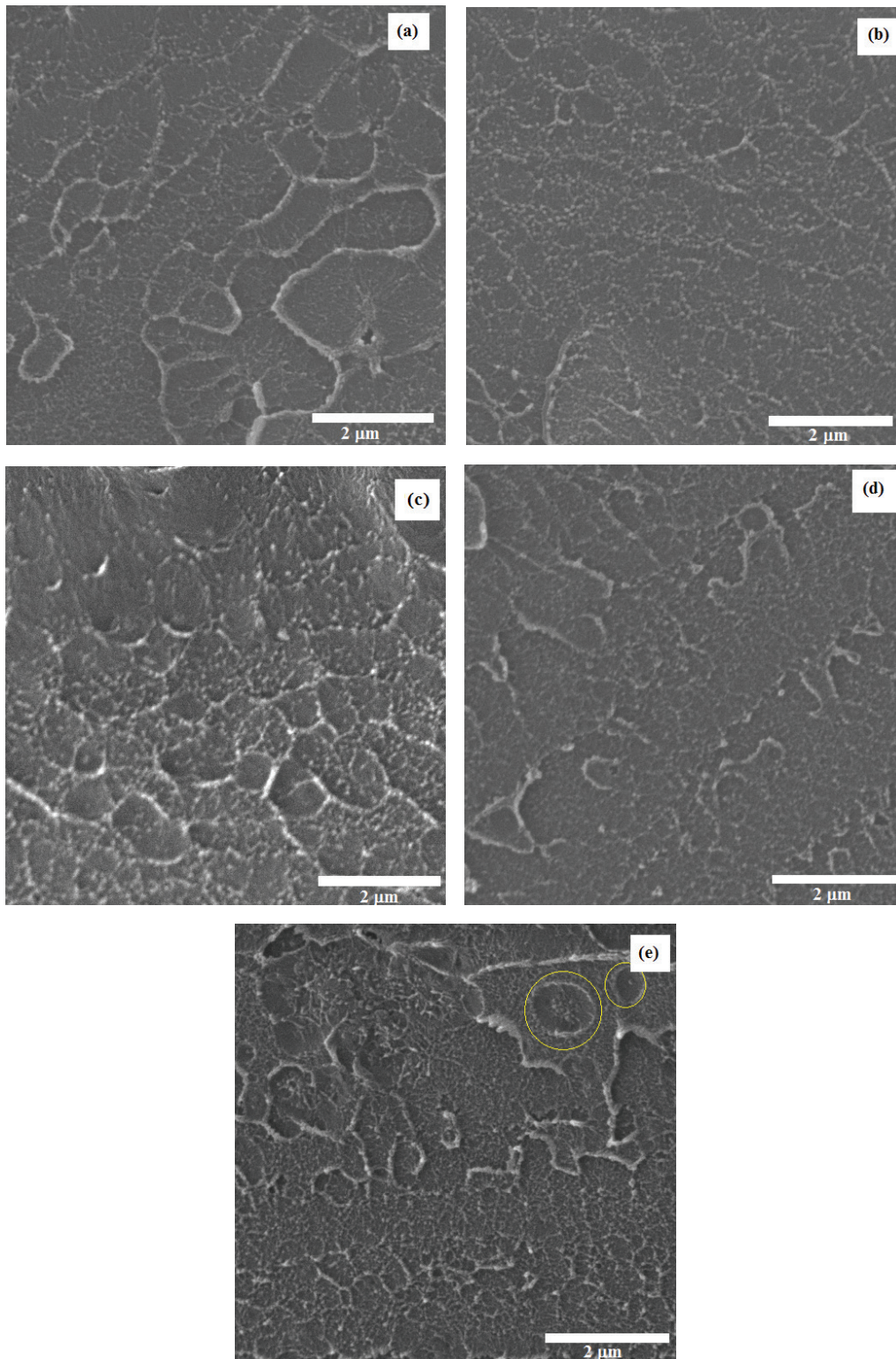


Fig. 9. Cross-sectional SEM images of the prepared P84/ZIF-8 (a) neat P84, (b) 2.5 wt%, (c) 5 wt%, (d) 7.5 wt% and (e) 10 wt%.

3.3.2. Comparison of present pervaporation performance with literature data

The results of PV performance of the prepared membranes were also compared with those of the various

membranes reported in literatures as shown in Table 2. As observed, the obtained enhancement in separation performance is comparable with the most reported results. Based on the literatures, compared with the neat membranes,

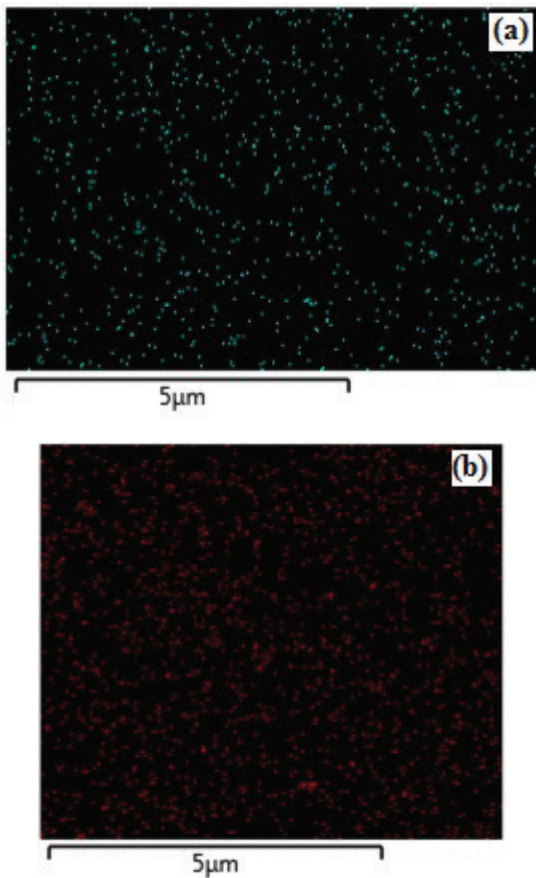


Fig. 10. EDX mapping for Zn from the cross-section of P84/ZIF-8 MMMs with different loadings of ZIF-8 (a) 2.5 wt% and (b) 7.5 wt%.

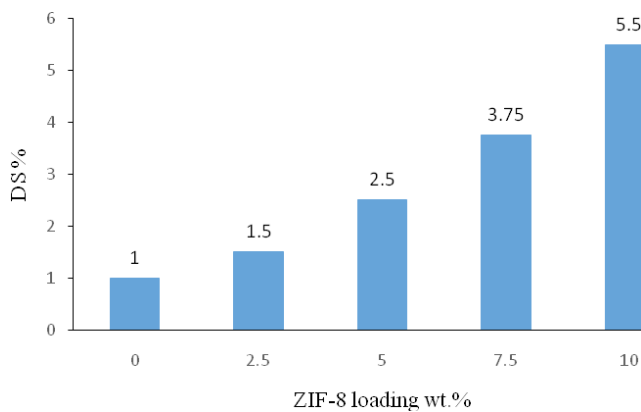


Fig. 11. Percentage DS of the prepared P84/ZIF-8 MMMs.

permeation flux and separation factor of MMMs change in ranges from –20% to 692% and from –92% to 282%, respectively. As observed, the P84 MMM with 5 wt% ZIF-8 loading shows about 11% increase in permeation flux without any decrease in separation factor, while, for most membranes presented in Table 2, by increasing permeation flux, their separation factor decreases [3,30–32,42]. The SEM image of this membrane does not show agglomeration

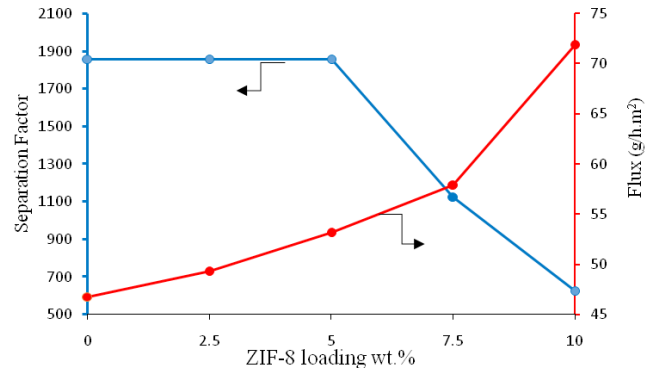


Fig. 12. Effect of ZIF-8 loading on PV performance of the prepared P84/ZIF-8 MMMs for dehydration of 85 wt% IPA aqueous solution at 25°C.

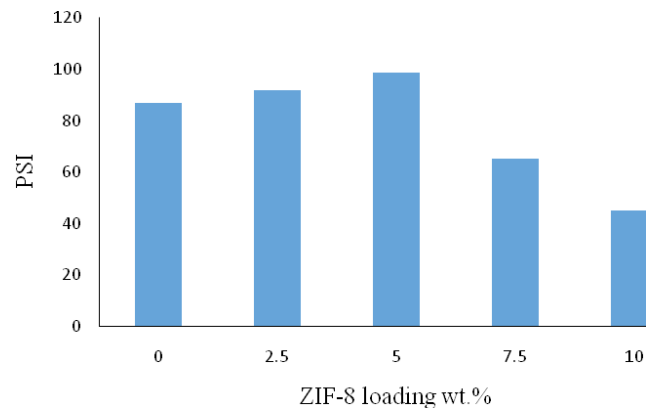


Fig. 13. Effect of ZIF-8 loading on PSI of different P84/ZIF-8 MMMs.

of the ZIF-8 nanoparticles. Thus, good adhesion between the ZIF-8 nanoparticles and the P84 matrix may slightly increase permeation flux without any reduction in separation factor. But, at higher ZIF-8 loadings due to the interfacial voids and the ZIF-8 nanoparticles agglomeration separation factor decreases dramatically.

4. Conclusion

In this study, ZIF-8 nanoparticles were dispersed in P84 matrix directly to prepare MMMs for dehydration of IPA. MMMs with ZIF-8 contents of 2.5, 5, 7.5 and 10 wt% were prepared. SEM images showed that ZIF-8 nanoparticles well disperse in the polymer matrix and only at high ZIF-8 loading the nanoparticles are aggregated. By increasing the ZIF-8 loading up to 5 wt%, total flux increases slightly without any reduction in separation factor. However, by increasing the ZIF-8 loading to 7.5 and 10 wt% because of agglomeration of the ZIF-8 nanoparticles, separation factor decreases extremely. This performance indicates that ZIF-8 and P84 have poor compatibility which needs to be improved by modification methods. The MMM with 5 wt% ZIF-8 loading exhibits the highest PSI value compared with the other synthesized membranes and the best performance for PV dehydration of IPA.

Table 2

Comparative study of PV performance of the prepared MMMs with the MMMs reported in the literatures for dehydration of IPA

| Polymer | Filler | Feed IPA concentration (wt%) | Temperature (°C) | Loading (wt%) | Neat membrane performance | | MMM membrane performance | | Reference |
|-----------------------|------------------------------------|------------------------------|------------------|---------------|---------------------------|----------|--------------------------|----------|---------------|
| | | | | | J (g/m ² h) | α | J (g/m ² h) | α | |
| Matrimid | Zeolite 4A | 90 | 30 | 15 | 13.6 | 1,290 | 21 | >5,000 | [43] |
| Matrimid | Cu ₃ (BTC) ₂ | 90 | 50 | 30 | 240 | 260 | 400 | 245 | [32] |
| Matrimid | MgO | 82 | 100 | 15 | 150 | 600 | 120 | 1,200 | [16] |
| Polyimide (BAPP–BODA) | Zeolite 13X | 90 | 25 | 33.3 | 90 | 158 | 150 | 272 | [35] |
| PBI | ZIF-8 | 85 | 60 | 33.7 | 13 | >5,000 | 103 | 1,686 | [31] |
| PVA | ZIF-8 | 90 | 30 | 5 | 135 | 163 | 870 | 133 | [30] |
| P84 | Zeolite 13X | 85 | 60 | 40 | 30 | 3,000 | 110 | 2,700 | [42] |
| P84 | Zeolite 5A | 85 | 60 | 20 | 30 | 3,000 | 40 | 4,200 | [42] |
| P84 | ZIF-90 | 85 | 60 | 30 | 49 | >5,000 | 114 | 385 | [3] |
| NaAlg | <i>p</i> -TSA treated clay | 10 | 30 | 10 | 1,734 (GPU) | 244 | 3,423 (GPU) | >5,000 | [44] |
| P84 | ZIF-8 | 85 | 25 | 5 | 46 | 1,858 | 51 | 1,858 | Present study |

References

- [1] E. Okumus, T. Gurkan, L. Yilmaz, Development of a mixed-matrix membrane for pervaporation, *Sep. Sci. Technol.*, 29 (1994) 2451–2473.
- [2] N.R. Singha, S. Kar, S. Ray, S.K. Ray, Separation of isopropyl alcohol–water mixtures by pervaporation using crosslink IPN membranes, *Chem. Eng. Process*, 48 (2009) 1020–1029.
- [3] D. Hua, Y.K. Ong, Y. Wang, T. Yang, T.-S. Chung, ZIF-90/P84 mixed matrix membranes for pervaporation dehydration of isopropanol, *J. Membr. Sci.*, 453 (2014) 155–167.
- [4] J.J. Alcaraz-Espinoza, A.E. Chávez-Guajardo, J.C. Medina-Llamas, C.A.S. Andrade, C.P. de Melo, Hierarchical composite polyaniline–(electrospun polystyrene) fibers applied to heavy metal remediation, *ACS Appl. Mater. Interfaces*, 7 (2015) 7231–7240.
- [5] K.R. Reddy, M. Hassan, V.G. Gomes, Hybrid nanostructures based on titanium dioxide for enhanced photocatalysis, *Appl. Catal., A*, 489 (2015) 1–16.
- [6] S.-Y. Huang, C.-S. Fan, C.-H. Hou, Electro-enhanced removal of copper ions from aqueous solutions by capacitive deionization, *J. Hazard. Mater.*, 278 (2014) 8–15.
- [7] K.R. Reddy, K. Nakata, T. Ochiai, T. Murakami, D.A. Tryk, A. Fujishima, Facile fabrication and photocatalytic application of Ag nanoparticles–TiO₂ nanofiber composites, *J. Nanosci. Nanotechnol.*, 11 (2011) 3692–3695.
- [8] A.M. Showkat, Y.-P. Zhang, M.S. Kim, A.I. Gopalan, K.R. Reddy, K. Lee, Analysis of heavy metal toxic ions by adsorption onto amino-functionalized ordered mesoporous silica, *Bull. Korean Chem. Soc.*, 28 (2007) 1985–1992.
- [9] S. Mosleh, T. Khosravi, O. Bakhtiari, T. Mohammadi, Zeolite filled polyimide membranes for dehydration of isopropanol through pervaporation process, *Chem. Eng. Res. Des.*, 90 (2012) 433–441.
- [10] Y. Bai, L. Dong, C. Zhang, J. Gu, Y. Sun, L. Zhang, H. Chen, ZIF-8 filled polydimethylsiloxane membranes for pervaporative separation of *n*-butanol from aqueous solution, *Sep. Sci. Technol.*, 48 (2013) 2531–2539.
- [11] J. Yu, H. Li, H. Liu, Recovery of acetic acid over water by pervaporation with a combination of hydrophobic ionic liquids, *Chem. Eng. Commun.*, 193 (2006) 1422–1430.
- [12] A.C. Duque Salazar, M.Á. Gómez García, J. Fontalvo, M. Jedrzejczyk, J.M. Rynkowski, I. Dobrosz-Gómez, Ethanol dehydration by pervaporation using microporous silica membranes, *Desal. Wat. Treat.*, 51 (2013) 2368–2376.
- [13] M. Peydayesh, S. Asarehpour, T. Mohammadi, O. Bakhtiari, Preparation and characterization of SAPO-34 – Matrimid® 5218 mixed matrix membranes for CO₂/CH₄ separation, *Chem. Eng. Res. Des.*, 91 (2013) 1335–1342.
- [14] L.Y. Jiang, Y. Wang, T.-S. Chung, X.Y. Qiao, J.-Y. Lai, Polyimides membranes for pervaporation and biofuels separation, *Prog. Polym. Sci.*, 34 (2009) 1135–1160.
- [15] C.M. Zimmerman, A. Singh, W.J. Koros, Tailoring mixed matrix composite membranes for gas separations, *J. Membr. Sci.*, 137 (1997) 145–154.
- [16] L.Y. Jiang, T.-S. Chung, R. Rajagopalan, Matrimid®/MgO mixed matrix membranes for pervaporation, *AIChE J.*, 53 (2007) 1745–1757.
- [17] Y. Niu, X. Zhang, J. Zhao, Y. Tian, X. Yan, Y. Li, Fabrication, structure and mechanism of reduced graphene oxide-based carbon composite films, *J. Mater. Chem. A*, 2 (2014) 10502–10507.
- [18] S.J. Han, H.-I. Lee, H.M. Jeong, B.K. Kim, A.V. Raghu, K.R. Reddy, Graphene modified lipophilically by stearic acid and its composite with low density polyethylene, *J. Macromol. Sci.*, 53 (2014) 1193–1204.
- [19] M. Hassan, K.R. Reddy, E. Haque, A.I. Minett, V.G. Gomes, High-yield aqueous phase exfoliation of graphene for facile nanocomposite synthesis via emulsion polymerization, *J. Colloid Interface Sci.*, 410 (2013) 43–51.
- [20] Y.P. Zhang, S.H. Lee, K.R. Reddy, A.I. Gopalan, K.P. Lee, Synthesis and characterization of core-shell SiO₂ nanoparticles/poly (3-aminophenylboronic acid) composites, *J. Appl. Polym. Sci.*, 104 (2007) 2743–2750.
- [21] S.H. Choi, D.H. Kim, A.V. Raghu, K.R. Reddy, H.-I. Lee, K.S. Yoon, H.M. Jeong, B.K. Kim, Properties of graphene/waterborne polyurethane nanocomposites cast from colloidal dispersion mixtures, *J. Macromol. Sci.*, 51 (2012) 197–207.
- [22] K.R. Reddy, B.C. Sin, K.S. Ryu, J.-C. Kim, H. Chung, Y. Lee, Conducting polymer functionalized multi-walled carbon nanotubes with noble metal nanoparticles: synthesis, morphological characteristics and electrical properties, *Synth. Met.*, 159 (2009) 595–603.
- [23] K.M. Gheimasi, M. Peydayesh, T. Mohammadi, O. Bakhtiari, Prediction of CO₂/CH₄ permeability through Sigma-1–Matrimid®5218 MMMs using the Maxwell model, *J. Membr. Sci.*, 466 (2014) 265–273.
- [24] K. Mohammad Gheimasi, T. Mohammadi, O. Bakhtiari, Modification of ideal MMMs permeation prediction models:

- effects of partial pore blockage and polymer chain rigidification, *J. Membr. Sci.*, 427 (2013) 399–410.
- [25] R. Pal, New models for thermal conductivity of particulate composites, *J. Reinf. Plast. Compos.*, 26 (2007) 643–651.
- [26] B. Zornoza, C. Tellez, J. Coronas, J. Gascon, F. Kapteijn, Metal organic framework based mixed matrix membranes: an increasingly important field of research with a large application potential, *Microporous Mesoporous Mater.*, 166 (2013) 67–78.
- [27] B. Baheri, M. Shahverdi, M. Rezakazemi, E. Motaei, T. Mohammadi, Performance of PVA/NaA mixed matrix membrane for removal of water from ethylene glycol solutions by pervaporation, *Chem. Eng. Commun.*, 202 (2014) 316–321.
- [28] P. Peng, B. Shi, Y. Lan, A review of membrane materials for ethanol recovery by pervaporation, *Sep. Sci. Technol.*, 46 (2010) 234–246.
- [29] Y. Wu, H. Tan, D. Zhang, T. Li, Pervaporation of acetaldehyde aqueous solution through zeolite 3A-polyurethane (PU) composite membrane, *Sep. Sci. Technol.*, 46 (2011) 1908–1914.
- [30] M. Amirilargani, B. Sadatnia, Poly(vinyl alcohol)/zeolitic imidazolate frameworks (ZIF-8) mixed matrix membranes for pervaporation dehydration of isopropanol, *J. Membr. Sci.*, 469 (2014) 1–10.
- [31] G.M. Shi, T. Yang, T.S. Chung, Polybenzimidazole (PBI)/zeolitic imidazolate frameworks (ZIF-8) mixed matrix membranes for pervaporation dehydration of alcohols, *J. Membr. Sci.*, 415–416 (2012) 577–586.
- [32] S. Sorribas, A. Kudasheva, E. Almendro, B. Zornoza, Ó. de la Iglesia, C. Tellez, J. Coronas, Pervaporation and membrane reactor performance of polyimide based mixed matrix membranes containing MOF HKUST-1, *Chem. Eng. Sci.*, 124 (2015) 37–44.
- [33] S. Liu, G. Liu, X. Zhao, W. Jin, Hydrophobic-ZIF-71 filled PEBA mixed matrix membranes for recovery of biobutanol via pervaporation, *J. Membr. Sci.*, 446 (2013) 181–188.
- [34] C.-H. Kang, Y.-F. Lin, Y.-S. Huang, K.-L. Tung, K.-S. Chang, J.-T. Chen, W.-S. Hung, K.-R. Lee, J.-Y. Lai, Synthesis of ZIF-7/chitosan mixed-matrix membranes with improved separation performance of water/ethanol mixtures, *J. Membr. Sci.*, 438 (2013) 105–111.
- [35] C.-L. Li, S.-H. Huang, W.-S. Hung, S.-T. Kao, D.-M. Wang, Y. Jean, K.-R. Lee, J.-Y. Lai, Study on the influence of the free volume of hybrid membrane on pervaporation performance by positron annihilation spectroscopy, *J. Membr. Sci.*, 313 (2008) 68–74.
- [36] J. Cravillon, S. Münzer, S.-J. Lohmeier, A. Feldhoff, K. Huber, M. Wiebcke, Rapid room-temperature synthesis and characterization of nanocrystals of a prototypical zeolitic imidazolate framework, *Chem. Mater.*, 21 (2009) 1410–1412.
- [37] Z. Zhang, S. Xian, H. Xi, H. Wang, Z. Li, Improvement of CO₂ adsorption on ZIF-8 crystals modified by enhancing basicity of surface, *Chem. Eng. Sci.*, 66 (2011) 4878–4888.
- [38] J.A. Thompson, K.W. Chapman, W.J. Koros, C.W. Jones, S. Nair, Sonication-induced Ostwald ripening of ZIF-8 nanoparticles and formation of ZIF-8/polymer composite membranes, *Microporous Mesoporous Mater.*, 158 (2012) 292–299.
- [39] Z.Y. Li, W.M. Lam, C. Yang, B. Xu, G.X. Ni, S.A. Abbah, K.M.C. Cheung, K.D.K. Luk, W.W. Lu, Chemical composition, crystal size and lattice structural changes after incorporation of strontium into biomimetic apatite, *Biomaterials*, 28 (2007) 1452–1460.
- [40] Y. Pan, Y. Liu, G. Zeng, L. Zhao, Z. Lai, Rapid synthesis of zeolitic imidazolate framework-8 (ZIF-8) nanocrystals in an aqueous system, *Chem. Commun.*, 47 (2011) 2071–2073.
- [41] Y. Shen, A.C. Lua, Structural and transport properties of BTDA-TDI/MDI co-polyimide (P84)–silica nanocomposite membranes for gas separation, *Chem. Eng. J.*, 188 (2012) 199–209.
- [42] X. Qiao, T.-S. Chung, R. Rajagopalan, Zeolite filled P84 co-polyimide membranes for dehydration of isopropanol through pervaporation process, *Chem. Eng. Sci.*, 61 (2006) 6816–6825.
- [43] T. Khosravi, S. Mosleh, O. Bakhtiari, T. Mohammadi, Mixed matrix membranes of Matrimid 5218 loaded with zeolite 4A for pervaporation separation of water–isopropanol mixtures, *Chem. Eng. Res. Des.*, 90 (2012) 2353–2363.
- [44] D.P. Suhas, T.M. Aminabhavi, A.V. Raghu, *para*-Toluene sulfonic acid treated clay loaded sodium alginate membranes for enhanced pervaporative dehydration of isopropanol, *Appl. Clay Sci.*, 101 (2014) 419–429.